

Cylindrical Brushes of Comb Copolymer Molecules Containing Rigid Side Chains

Andrei Subbotin,^{†,‡} Mika Saariaho,[§] Roman Stepanyan,[†] Olli Ikkala,[§] and Gerrit ten Brinke^{*,†,§}

Laboratory of Polymer Chemistry and Materials Science Center, University of Groningen, Nijenborgh 4, 9747 AG, Groningen, The Netherlands; Institute of Petrochemical Synthesis, Russian Academy of Sciences, Moscow 117912, Russia; and Department of Engineering Physics and Mathematics, Materials, Physics Laboratory, Helsinki University of Technology, P.O. BOX 2200, FIN-02015 HUT, Espoo, Finland

Received February 10, 2000; Revised Manuscript Received June 1, 2000

ABSTRACT: An analysis of the cylindrical brush of an isolated comb copolymer molecule, consisting of a semiflexible backbone and rodlike side chains, is presented. Using a mean-field approach and a simplifying assumption, which is tested by computer simulations, we find that the persistence length of the brush, λ , scales as $\lambda \propto L^2/\ln L$ for large values of the side chain length L . In the cylindrical brush regime the order parameter of the rods is negative, implying that the rods orient normal to the cylindrical axis.

I. Introduction

In this paper, we consider theoretically the conformational behavior of cylindrical comb copolymer brushes in dilute solution for the specific case of rigid rod side chains. Cylindrical comb copolymer brushes are defined here as long chain molecules consisting of a flexible backbone densely grafted with relatively long side chains which may either be flexible or rigid. A related class, which also attracted considerable attention lately, are “hairy rod” polymers, consisting of a rigid backbone densely grafted with flexible side chains.¹ The interest in cylindrical comb copolymer brushes is directly related to the possibility to form stiff cylindrical “shape persistent” structures based exclusively on the intramolecular excluded volume interactions. Obviously, from this perspective, “hairy rod” molecules are not of direct interest.

Research on cylindrical comb copolymer brushes began very recently; however, a large number of experimental,^{2–20} computational,^{21–32} and theoretical studies^{33–35} have already been devoted to this subject. In the early experimental studies of the late 1970s, Roovers and co-workers^{2–4} synthesized a series of long-chain comb copolymers and characterized their size relative to linear chains of the same molecular weight using several techniques. The grafting density of the molecules was low, and the stiffness, i.e., the persistence length, of the comb copolymer was not considered in any detail. A major breakthrough in synthetic methods was achieved 10 years later by Tsukahara et al.⁵ who succeeded in homopolymerization of macromonomers of anionically prepared oligostyrenes ($700 \leq M_n \leq 5000$) and obtained degrees of polymerization of up to 1000. The structural studies^{5–7,14} revealed that in a dilute good solvent the main chain of the molecules exhibits an almost rodlike conformation characterized by a persistence length of up to $\lambda = 1000$ Å. For polymer concentrations of 30 wt % and higher, a very narrow

X-ray scattering peak was observed, interpreted as evidence for lyotropic behavior. Recently, a large number of experimental studies^{3–14} on cylindrical comb copolymer brushes following the synthetic route developed by Tsukahara⁵ have been published, all confirming the presence of strongly extended conformations of these molecules in a dilute good solvent. The latests examples involve rod–comb copolymers¹⁵ as well as structures having dendrons as side chains.^{16,17}

Recently, we presented the first off-lattice Monte Carlo computer simulations on conformations of isolated comb copolymer brushes with a very high density of relatively long side chains.^{21–25} A few related systems have been investigated by other researchers.^{26–32} In particular, the recent lattice studies by Rouault,³¹ cooperating in part with Borisov,²⁶ focused on cylindrical comb copolymer brushes large enough to have side chains obeying scaling behavior. However, the issue of persistence length was not pursued. Our off-lattice simulations addressed structures with an effectively higher coverage of the side chains and thus a much stronger excluded volume effect between successive side chains. We considered two essentially different cases corresponding to either flexible or rigid rod side chains. In relation to possible lyotropic behavior of these structures, the essential parameter is the ratio λ/D between persistence length and diameter of the brush.^{36,37} In our computer simulation studies the behavior of λ/D as a function of side chain length was discussed in some detail and can be summarized as follows. In the case of flexible side chains, λ/D was essentially constant as a function of the number of beads M in the side chains for values up to $M = 80$. In the case of rigid rod side chains, on the other hand, $\lambda/D \propto L$, where L is the length of the side chains. In both cases the backbone consisted of 300 beads freely jointed together to which 150 side chains were grafted consisting of beads of equal size as the backbone, either freely jointed (flexible side chain) or jointed with a fixed bond angle of 180° (rigid rod side chains).

The theory of polymer brushes, cylindrical comb copolymer brushes, and polymers grafted to convex

[†] University of Groningen.

[‡] Russian Academy of Sciences.

[§] Helsinki University of Technology.

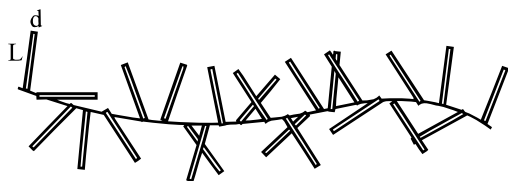


Figure 1. Model of comb copolymer molecule with rigid side chains.

surfaces has received a lot of attention as well^{26,33–35,38–45} However, the complex molecular architecture of cylindrical comb copolymer brushes has made a comprehensive description of their conformational behavior quite a challenging problem. Clearly, opposite views concerning the conformation in dilute good solvent have been put forward,^{34,35} based on the Daoud–Cotton model.³⁸ In the case of molecules with fully flexible side chains of length M , Birshtein and co-workers predicted³⁵ more than a decade ago that the persistence length λ is proportional to the diameter of the brush, which implies that the ratio λ/D is independent of the side chain length. In contrast, Fredrickson³⁴ published a scaling analysis of the same problem, reaching a quite different conclusion of $\lambda/D \propto M^{9/8}$. Our most recent theoretical self-consistent treatment led to $\lambda/D \propto M^{6/4}$, in agreement with the last result.³³ Our current understanding is that the discrepancy between this prediction and our computer simulation data is due to the fact that even for side chain lengths of $M = 80$ and the high grafting density used, we are still not in the scaling regime. Now, to complete the picture, we present here the analysis of cylindrical comb copolymer brushes involving rigid rod side chains.

Although the theoretical model considered is slightly different from the case investigated by recent simulations²⁵ (there is no excluded volume of the backbone in the theory) it is possible to compare the results in the regime of large side chain length (or high grafting densities) where the properties of the backbone are relatively unimportant.

II. Straight Cylindrical Brush

In the present paper, we consider comb copolymer molecules having rodlike side chains of length L and diameter d , $L \gg d$, Figure 1. We assume that the backbone is a semiflexible chain of contour length L_c and persistence length λ_0 , containing N grafted rods with a distance b between two consecutive grafting points, satisfying $d \ll b < \lambda_0$, and $L_c = Nb$. We will also assume that the rod length $L \gg b$.

Our considerations start with a straight cylindrical brush. First, we calculate the free energy per rod in this regime, and after that, we will calculate the free energy due to bending of the brush and thus obtain the persistence length.

The free energy of the rod consists of two parts, namely the orientational free energy and the steric free energy.^{36,37,46,47} To find the steric free energy, we use a mean-field approach. According to this approach the steric part of the free energy equals, $F_{\text{ster}} \approx k_B T \ln(4\pi/\Omega)$, where Ω is the average volume in orientation space available for a test rod when the other rods are fixed in their average positions. Let us introduce a system of coordinates as illustrated in Figure 2, where the z axis is directed along the axis of the cylinder and the (x, y) plane corresponds to the cross-section. The corresponding spherical angles (θ, φ) are defined in the usual way,

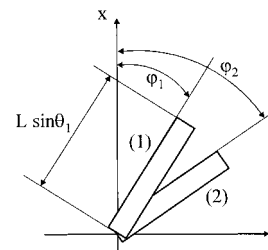
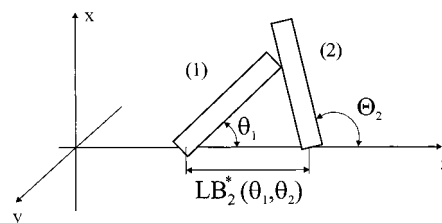


Figure 2. Schematic illustration of the interaction between two rods for a straight brush.

so that θ is the angle between the rod and the z axis and φ is the azimuth angle. If the test rod has polar angle θ_1 and azimuth φ_1 , then it can interact with another rod having polar angle θ_2 and azimuth φ_2 only if $\varphi_1 \approx \varphi_2$ (here we use the fact that $d/b \ll 1$ and assume that the angles $\theta_1, \theta_2 > d/b$) and if their distance is smaller than a critical value $LB_2^*(\theta_1, \theta_2)$ (Figure 2). Here $B_2^*(\theta_1, \theta_2)$ is a geometrical factor, which for $0 < \theta_1 < \pi/2$ is given by

$$B_2^*(\theta_1, \theta_2) = \begin{cases} \cos \theta_2 - \sin \theta_2 \cot \theta_1, & 0 < \theta_2 < \theta_1 \\ \cos \theta_1 - \sin \theta_1 \cot \theta_2, & \theta_1 < \theta_2 < \pi - \theta_1 \\ \sin \theta_2 \cot \theta_1 - \cos \theta_2, & \pi - \theta_1 < \theta_2 < \pi \end{cases} \quad (1)$$

and for $\pi/2 < \theta_1 < \pi$ can be found by symmetry. The range of the interaction between the rods in the brush is therefore of the order of L .

When the test rod, denoted by 1, and another rod, denoted by 2, are a distance $z < LB_2^*(\theta_1, \theta_2)$ apart, the excluded azimuth angle, $\psi_z(\theta_1, \theta_2)$, for the test rod due to this second rod can be found using a simple geometric picture (Figure 2):

$$\psi_z(\theta_1, \theta_2) \approx \frac{2d}{z} |\cot \theta_1 - \cot \theta_2| \quad (2)$$

Let us introduce the distribution function of rod orientations, $f(\mathbf{n})$, where \mathbf{n} is the orientation vector of the rod. $f(\mathbf{n})$ satisfies the normalization condition $\int d\mathbf{n} f(\mathbf{n}) = 1$ and should be found after minimization of the free energy. The probability $p_z(\theta_1, \varphi_1)$ that the test rod does not interact with the rod 2 is

$$p_z(\theta_1, \varphi_1) = 1 - \int d\mathbf{n}_2 f(\mathbf{n}_2) \delta(\varphi_1 - \varphi_2) \psi_z(\theta_1, \theta_2) \quad (3)$$

Multiplying the probabilities $p_z(\theta_1, \varphi_1)$ for different positions z of the given rods, which may interact with the test rod, we can find the probability $P(\theta_1, \varphi_1)$ that the test rod does not interact with any rod:

$$P(\theta_1, \varphi_1) = \prod_{\{z\}} (1 - \int d\mathbf{n}_2 f(\mathbf{n}_2) \delta(\varphi_1 - \varphi_2) \psi_z(\theta_1, \theta_2)) \quad (4)$$

Averaging further the function $P(\theta_1, \varphi_1)$ with respect

to the angles θ_1 , φ_1 , we find the average available free volume Ω for the test rod in orientation space from the formula

$$\Omega \simeq 4\pi \int d\mathbf{n}_1 f(\mathbf{n}_1) P(\mathbf{n}_1) \quad (5)$$

In the present formulation, the problem is very complicated mathematically because the angular range for θ_2 in the integral of eqs 3 and 4 depends on the distance z and θ_1 . To simplify the calculations, we assume that $\theta_2 = \pi/2$; i.e., we estimate the excluded azimuth for the test rod by another rod by assuming the latter to be oriented perpendicular to the cylinder axis (computer simulation data supporting this assumption are given further on). In this case the product in eq 4 should be taken over the positions $z = kb$, $k = 1, \dots, n^*$, of the different interacting rods, where $n^* = (L/b) \cos \theta_1$ is the maximum number of rods interacting with the test rod. Thus, using eqs 2–5 and taking into account that the distribution function does not depend on φ due to symmetry, eq 5 can be written using the following approximation

$$\frac{\Omega}{4\pi} \simeq \int d\mathbf{n}_1 f(\mathbf{n}_1) \prod_{k=1}^{n^*} \left(1 - \frac{\Delta\psi_k}{2\pi}\right) \simeq \exp\left(-\frac{1}{2\pi} \int d\mathbf{n}_1 f(\mathbf{n}_1) \sum_{k=1}^{n^*} \Delta\psi_k\right) \quad (6)$$

where

$$\Delta\psi_k \simeq \frac{2d}{bk} |\cot \theta_1| \quad (7)$$

Hence, the steric part of the free energy is

$$F_{\text{steric}} \simeq \frac{k_B T}{2\pi} \int d\mathbf{n}_1 f(\mathbf{n}_1) \sum_{k=1}^{n^*} \Delta\psi_k \simeq \frac{k_B T d}{\pi b} \ln(n^*) \int d\mathbf{n}_1 f(\mathbf{n}_1) |\cot \theta_1| \quad (8)$$

Because n^* occurs as argument of the logarithmic function, we approximate n^* as $n^* \simeq L/b$. The total free energy of the rod includes also the orientational entropy and therefore is given by

$$\frac{F_{\text{rod}}}{k_B T} = \int f(\mathbf{n}) \ln f(\mathbf{n}) d\mathbf{n} + \frac{d}{\pi b} \ln(L/b) \int d\mathbf{n} f(\mathbf{n}) |\cot \theta| \quad (9)$$

Minimization of the free energy eq 9 using the normalization condition for the distribution function $f(\mathbf{n})$, which here due to symmetry does not depend on φ , gives rise to the following equation

$$\ln(f(\mathbf{n})/\Lambda) = -\epsilon |\cot \theta| \quad (10)$$

where

$$\epsilon = \frac{d}{\pi b} \ln(L/b) \quad (11)$$

Hence, the distribution function is given by

$$f(\mathbf{n}) = \Lambda \exp(-\epsilon |\cot \theta|) \quad (12)$$

where Λ is the normalization constant. The free energy equation follows from eqs 9 and 12:

$$F_{\text{rod}} = k_B T \ln \Lambda \quad (13)$$

Since Λ cannot be found analytically in the general case, we will consider two limiting cases. The first one corresponds to $\epsilon \ll 1$ (regime 1). In this case we use the perturbation theory and expand the distribution function in the series with respect to the small parameter ϵ . In the first order of the perturbation scheme

$$f(\mathbf{n}) \simeq \Lambda (1 - \epsilon |\cot \theta|) \quad (14)$$

and

$$\Lambda \simeq \frac{1}{4\pi} (1 + \epsilon) \quad (15)$$

Note, the perturbation scheme does not work for the angles $\theta \leq \epsilon$. Moreover, the rods are repelled from this angle zone. The orientational order parameter can be calculated using the distribution function eq 14 excluding the smallest angles, and is slightly negative

$$\eta = \frac{1}{2} \langle 3 \cos^2 \theta - 1 \rangle \simeq -\frac{\epsilon}{2} \simeq -\frac{1}{2\pi} \frac{d}{b} \ln(L/b) \quad (16)$$

The free energy per rod can be found from eqs 11, 13, and 15 and equals

$$F_{\text{rod}} \simeq \frac{k_B T d}{\pi b} \ln(L/b) \quad (17)$$

In order that this mean field picture be correct, the fluctuations of the backbone orientation, $\delta\theta$, on the scales of the order of b and L should be smaller than ϵ . Generally the persistence length is different on the scale $\sim b$ and $\sim L$ due to interactions between the side rods, therefore we should distinguish two cases. The persistence length on the scale $\sim b$ equals λ_0 ; therefore, the first inequality implies that $\delta\theta(b) \simeq \sqrt{b/\lambda_0} \ll \epsilon$, or $\lambda_0 \gg b(b/d)^2$ which we assume to be fulfilled. The second condition will be considered in the next section, after estimation of the corresponding persistence length.

Next we proceed to the case $\epsilon \gg 1$ (regime 2). Here, the distribution function is given by

$$f(\mathbf{n}) = \Lambda \exp\left(-\epsilon \left|\frac{\pi}{2} - \theta\right|\right) \quad (18)$$

with the normalization constant $\Lambda = \epsilon/(4\pi)$. The orientational order parameter is negative

$$\eta = \frac{1}{2} \langle 3 \cos^2 \theta - 1 \rangle = -\frac{1}{2} + \frac{3\pi^2 b^2}{d^2 \ln^2(L/b)} \quad (19)$$

Hence, the rods have a tendency to orient perpendicular to the backbone. The free energy of the rod can again be estimated from eq 13

$$F \simeq k_B T \ln [(d/b) \ln(L/b)] \quad (20)$$

To support the approximation made in this section, we will compare the theoretical results from eqs 12 and 16 to simulation results. Conformations of a straight brush were studied by off-lattice Monte Carlo simulations. The simulations algorithm is thoroughly described in refs 22–25. The molecules consisted of a phantom straight

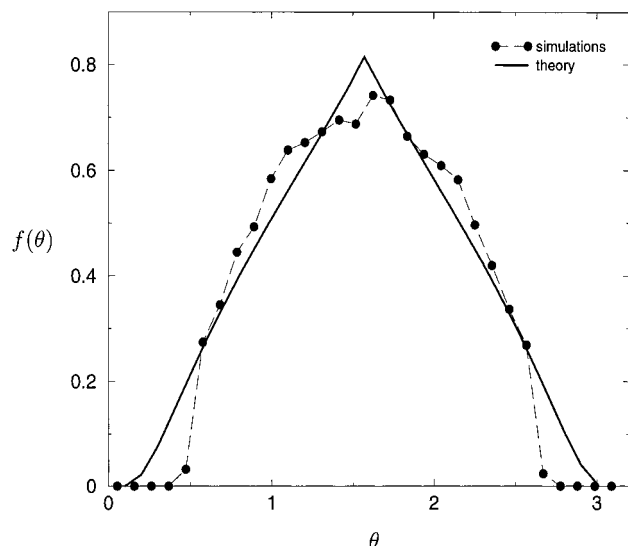


Figure 3. Distribution function $f(\theta)$ for $L = 200$ and $b = 2$.

backbone and rigid side chains modeled as a straight chain of hard spheres (beads). The diameter d of the beads was taken as the unit of length. Side chain lengths of up to 300 beads were considered. To suppress end effects all parameters of interest were computed by excluding one-sixth of the backbone from each end (backbone length was 300 for all simulation points except for $L = 200$ and 300 where the backbone consisted of 600 and 900 beads).

The initial conformation was formed as a 3D structure. The trial moves of the side chains consisted in choosing randomly new orientations and was always accepted if the new conformation did not cause an overlap between side chains. From the simulations the distribution function $f(\theta)$ and the order parameter η were obtained as a function of the distance b between successive grafting points and the length L of the side chain.

The distribution function for $b = 2$, $L = 200$ is shown in Figure 3. For these values of grafting density and length of side chains the parameter $\epsilon \approx 0.733$; i.e., it is still not in regime 2. Even though the simulation data show considerable scatter due to the long side chain involved, it is clear that the distribution function eq 12 and the simulation results are already in rather good agreement. The rods are excluded from the angular ranges $\theta \approx 0$ and $\theta \approx \pi$ due to their finite width. In the point $\theta = \pi/2$ the theoretical curve is not smooth as a result of the approximation.

Figure 4 presents the dependence of the order parameter η on the length of the rods for $b = 2$. Even for the largest value of L , ϵ does not satisfy the strong inequality $\epsilon \gg 1$ (for $L = 300$ $\epsilon = 0.797$) but extrapolation of the simulated data into the region of larger values of L demonstrates a rather good agreement with the theoretical result.

The results presented in Figures 3 and 4 show that the main assumption of $\theta_2 = \pi/2$, which simplified the calculations considerably, does not cause too large deviations. Also expression 19 implies that this assumption is valid for regime 2 ($\eta \approx -1/2$; i.e., all rods are oriented almost perpendicular to the backbone). However it is not valid for the first regime where $\eta \approx 0$ (see eq 16). Therefore, from here on this paper we will concentrate on the second regime which corresponds to

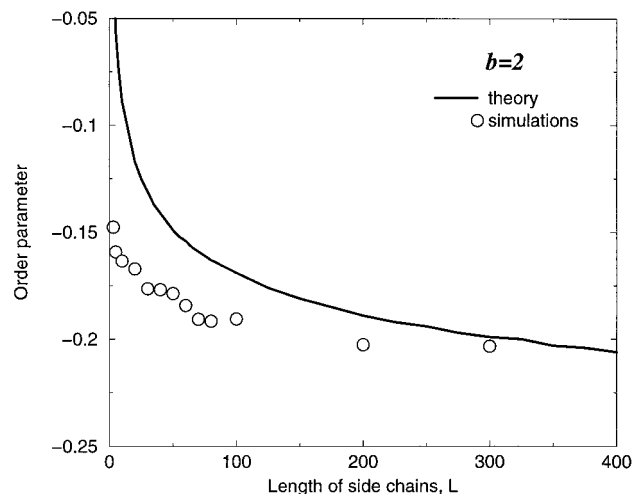


Figure 4. Order parameter as a function of length of rods for $b = 2$. The solid line is the theoretical curve, and points are result of simulations.

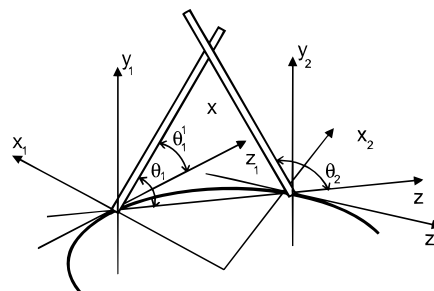


Figure 5. Interacting rods in a bent brush.

high grafting densities or long side chains and regime 1 will be considered only briefly using scaling arguments.

III. Bent Cylindrical Brush

Now we proceed to the calculation of the persistence length λ of the cylindrical brush, which can be achieved following a standard procedure.³⁴ If the cylindrical brush is homogeneously bent with a radius of curvature R , the free energy change is related to R and the persistence length λ by

$$\Delta F = k_B T \frac{\lambda L_c}{2R^2} \quad (21)$$

So, we will assume the brush to be bent with a radius of curvature R and calculate ΔF using the same methods as developed above. Let us consider two interacting rods and introduce three coordinate systems, connected with these rods (Figure 5). One of the coordinate systems we denote as Z . The z axis in this system is directed along the line connecting the grafting points of the rods, which we assume to be at a distance $z = kb$ apart (actually this distance is $kb(1 - (kb)^2/(24R^2))$, however the correction is numerically small and will be omitted). The x axis is perpendicular to the z axis and directed along the radius of curvature and the y axis is perpendicular to the (xz) plane. The other two coordinate systems are the local coordinate systems Z_i , $i = 1, 2$, defined in the following way. The origin of the local coordinate system coincides with the grafting point of the rod under consideration. The z_i axis is directed along the tangential line to the cylinder axis, and the $(x_i y_i)$ plane is

perpendicular to this axis and corresponds to the cross-section. The x_i axis is directed along the radius of curvature. Knowing the transformations between the basis unit vectors of the coordinate system Z , and the local coordinate systems Z_i , $i = 1, 2$, we can express the spherical angles (θ_1, φ_1) and (θ_2, φ_2) of rod 1 and rod 2 in the coordinate system Z through their local spherical coordinates $(\theta_1^1, \varphi_1^1)$ and $(\theta_2^2, \varphi_2^2)$ in the coordinate system Z_1 and Z_2 , respectively. This implies that the orientation vectors \mathbf{n}_1 , \mathbf{n}_2 are given by

$$\begin{aligned}\mathbf{n}_1 &= \cos \theta_1^1 \mathbf{e}_z^1 + \sin \theta_1^1 \cos \varphi_1^1 \mathbf{e}_x^1 + \sin \theta_1^1 \sin \varphi_1^1 \mathbf{e}_y^1 \\ &= \cos \theta_1 \mathbf{e}_z + \sin \theta_1 \cos \varphi_1 \mathbf{e}_x + \sin \theta_1 \sin \varphi_1 \mathbf{e}_y \quad (22)\end{aligned}$$

$$\begin{aligned}\mathbf{n}_2 &= \cos \theta_2^2 \mathbf{e}_z^2 + \sin \theta_2^2 \cos \varphi_2^2 \mathbf{e}_x^2 + \sin \theta_2^2 \sin \varphi_2^2 \mathbf{e}_y^2 \\ &= \cos \theta_2 \mathbf{e}_z + \sin \theta_2 \cos \varphi_2 \mathbf{e}_x + \sin \theta_2 \sin \varphi_2 \mathbf{e}_y \quad (23)\end{aligned}$$

The transformations between the basis unit vectors $(\mathbf{e}_z^i, \mathbf{e}_x^i, \mathbf{e}_y^i)$ of the coordinate system Z_i , $i = 1, 2$, and the basis vectors $(\mathbf{e}_z, \mathbf{e}_x, \mathbf{e}_y)$ of the coordinate system Z are the following

$$\mathbf{e}_z^1 = \cos(\theta^*/2) \mathbf{e}_z + \sin(\theta^*/2) \mathbf{e}_x \quad (24)$$

$$\mathbf{e}_x^1 = -\sin(\theta^*/2) \mathbf{e}_z + \cos(\theta^*/2) \mathbf{e}_x$$

$$\mathbf{e}_y^1 = \mathbf{e}_y$$

$$\mathbf{e}_z^2 = \cos(\theta^*/2) \mathbf{e}_z - \sin(\theta^*/2) \mathbf{e}_x \quad (25)$$

$$\mathbf{e}_x^2 = \sin(\theta^*/2) \mathbf{e}_z + \cos(\theta^*/2) \mathbf{e}_x$$

$$\mathbf{e}_y^2 = \mathbf{e}_y$$

where

$$\theta^*(z) = \frac{z}{R} \quad (26)$$

is the angle between the axis z_1 and z_2 . Using eqs 22–26 with a small parameter $\theta^*(z) \ll 1$, the angles θ_1 , φ_1 and θ_2 , φ_2 can be expressed in terms of the angles θ_1^1 , φ_1^1 , θ_2^2 , φ_2^2 , θ^* in the following way

$$\begin{aligned}\theta_1 &= \theta_1^1 + \frac{\theta^*}{2} \cos \varphi_1^1 + \frac{\theta^{*2}}{8} \cot \theta_1^1 \sin^2 \varphi_1^1; \\ \varphi_1 &= \varphi_1^1 - \frac{\theta^*}{2} \cot \theta_1^1 \sin \varphi_1^1 \quad (27)\end{aligned}$$

$$\begin{aligned}\theta_2 &= \theta_2^2 - \frac{\theta^*}{2} \cos \varphi_2^2 + \frac{\theta^{*2}}{8} \cot \theta_2^2 \sin^2 \varphi_2^2; \\ \varphi_2 &= \varphi_2^2 + \frac{\theta^*}{2} \cot \theta_2^2 \sin \varphi_2^2\end{aligned}$$

The interaction between the rods takes place when $\varphi_1 \approx \varphi_2$.

Now let us calculate the azimuth angle $\Delta\psi'_k(\theta_1^1, \varphi_1^1)$, which is excluded for the test rod 1 due to rod 2, when the last one is oriented perpendicular to the cylinder axis (i.e., we assume that $\theta_2^2 = \pi/2$), and the number of rods, which interact with the test rod is $n^{*'}(\theta_1^1, \varphi_1^1)$. Note that the excluded angles should be calculated in the local coordinate system Z_1 connected with the test

rod. The functions $\Delta\psi'_k$ and $n^{*'}$ can be found from geometrical arguments (Figure 5) and are given by

$$\Delta\psi'_k = \frac{2d(\cos \theta_1 - \sin \theta_1 \cot \theta_2)}{kb \sin \theta_1^1} \quad (28)$$

$$n^{*'} = \frac{L}{b} (\cos \theta_1 - \sin \theta_1 \cot \theta_2) \quad (29)$$

Here we assume that $0 \leq \theta_1^1 \leq \pi/2$, the case $\pi/2 \leq \theta_1^1 \leq \pi$ can be obtained by symmetry. In eqs 28, 29 we can eliminate the angles θ_1 , θ_2 using eq 27. After that the same procedure as before is followed to calculate the free energy. The calculations show that in this case the free energy is given by

$$\begin{aligned}\frac{F_{\text{rod}}}{k_B T} &= \int f(\mathbf{n}) \ln f(\mathbf{n}) d\mathbf{n} + \\ &\frac{d}{\pi b} \int d\mathbf{n} f(\mathbf{n}) \left[\ln(L/b) \left| \cot \theta \right| - \frac{2L}{R} \cos \varphi \left| \cos \theta \right| + \right. \\ &\left. \frac{L^2}{R^2} \left(\frac{3}{2} \cos^2 \varphi \sin \theta \left| \cos \theta \right| - \frac{9}{16} \cos^2 \theta \left| \cot \theta \right| \right) \right] \quad (30)\end{aligned}$$

where the distribution function $f(\mathbf{n})$ follows from minimization of the free energy. As it was mentioned before we consider region $\epsilon \gg 1$ (regime 2) where the approximation is valid. Using this distribution function, we can estimate the order parameter η' of the rods in the bent brush

$$\eta' = \eta + \frac{9}{4\epsilon^2 \ln(L/b)} \left(\frac{L}{R} \right)^2 \quad (31)$$

It is slightly increased compared to the straight brush, $\eta < \eta' < 0$, therefore rods become more disoriented.

After calculation of the integral in eq 30 in regime 2, we find that the correction to the free energy of the rod due to the bending is given by

$$\Delta F_{\text{rod}} \approx \frac{3k_B T}{4 \ln(L/b)} \left(\frac{L}{R} \right)^2 \quad (32)$$

The persistence length equals

$$\lambda \approx \lambda_0 + \frac{3}{2 \ln(L/b)} \frac{L^2}{b} \quad (33)$$

and scales as $\lambda \propto L^2/\ln L$ for large L . This scaling of the persistence length as a function of L is in good agreement with our recent computer simulations.²⁵

It is also possible to estimate the scaling behavior of the parameter λ/D : for $\epsilon \gg 1$ $D \propto L$ and therefore

$$\frac{\lambda}{D} \propto \frac{L}{\ln L} \propto L \quad (34)$$

which is in agreement with our computer simulations too.²⁵

Our assumption that the rods orient normal to the backbone cannot be used for calculation of the bent brush free energy in regime 1 ($\epsilon \ll 1$); therefore, let us use scaling arguments to consider this regime. Using eq 8 we obtain the potential energy of a rod in the straight brush, $U(\theta) \approx \epsilon |\cot \theta|$, where θ is the angle between the rod and the backbone. Upon bending this energy approximately equals $U(\theta, \varphi) \approx \epsilon |\cot \theta'(\theta)|$,

where $\theta' \approx \theta + \theta^*/2 \cos \varphi + \theta^{*2}/8 \cot \theta \sin^2 \varphi$ and θ^* is the characteristic bending angle of the backbone on the distance of the order of L , i.e., $\theta^* \approx L/R$ (see eqs 26, 27). After expansion of the function $U(\theta, \varphi)$ up to terms of the order of $1/R^2$ and averaging using the equilibrium distribution function eq 12 we find for the increase of the steric part of the free energy, $\Delta F_{\text{rod}} \sim k_B T(L/R)^2$. Therefore, the persistence length scales as $\lambda \sim L^2/b$ (more accurate consideration results in an additional logarithmic factor as in eq 33). Note, however, that this scaling result is valid only when the fluctuations of the backbone orientation on the length scale of the order of L are small, i.e., $\delta\theta(L) \approx \sqrt{L/\lambda} \ll \epsilon$, or when $L \gg L^* = b(b/d)^2$ for $b(b/d)^2 \ll \lambda_0 \ll b(b/d)^4$ and $L \gg L^* = b\sqrt{\lambda_0}/b$ for $\lambda_0 \gg b(b/d)^4$. The fluctuations become very important when the rod length $L < L^*$, and this regime is out of the scope of the present paper. Thus, our mean field result eq 33 is correct for side chain lengths $L \gg L^*$.

IV. Concluding Remarks

In the present paper, we calculated the persistence length λ of a cylindrical brush of a comb copolymer molecule consisting of a semiflexible backbone having a persistence length λ_0 with rigid side chains of length L and diameter d . The linear grafting density of the rods is $1/b$ so that $d \ll b \ll L$. Using a mean field approach we calculated the free energy both for a straight and a bent brush and found that the persistence length increases as a function of L and for large L scales as $\lambda \propto L^2/\ln L$. For short rods satisfying $L < L^* = b(b/d)^2$, the fluctuations become important and the mean field approach fails. Alternative approaches should be developed to calculate the persistence length in this case.

For low grafting density, or equivalently for short side chains ($L^* \ll L \ll b \exp(\pi b/d)$), in the straight brush regime the side chain rods are expelled from the angular range corresponding to parallel to the cylinder axis orientations and they are nearly isotropically distributed outside this range. With increasing grafting density or rod length, the rods orient in the direction normal to the cylinder axis. However, on bending the rods start to disorient and penetrate to the range with strong steric interaction and, therefore, the free energy increases. In this case the bending elasticity has the same nature as the Frank elasticity in liquid crystals.⁴⁸

In the present model we use a semiflexible backbone with persistence length λ_0 . However, in our computer simulations a slightly different model of a freely jointed hard sphere bead model was used for the backbone. Following Birshtein et al.³⁵ we can approximate the free energy of this kind of brush by adding to the free energy of rods attached to a "cylinder" (eq 20), the free energy due to stretching of the backbone. A simple calculation shows that the spatial distance between two successive grafting points is in a good approximation independent of the rod length, exactly as found in the computer simulations.²⁵

Acknowledgment. This research was supported by The Netherlands Organization for Scientific Research (NWO) as part of the Russian–Dutch research cooperation program.

References and Notes

- (1) Ballauf, M. *Angew. Chem. Int. Ed. Engl.* **1989**, *28*, 253.
- (2) Roovers, J. E. L. *Polymer* **1975**, *16*, 827.
- (3) Roovers, J. *Polymer* **1979**, *20*, 843.
- (4) Roovers, J.; Toporowski, P. M. *J. Polym. Sci., Polym. Phys. Ed.* **1980**, *18*, 1907.
- (5) Tsukahara, Y.; Tsutsumi, K.; Yamashita, Y.; Shimada, S. *Macromolecules* **1990**, *23*, 5201.
- (6) Tsukahara, Y.; Kohjiya, S.; Tsutsumi, K.; Okamoto, Y. *Macromolecules* **1994**, *27*, 1662.
- (7) Tsukahara, Y.; Ohta, Y.; Senoo, K. *Polymer* **1995**, *36*, 3413.
- (8) Wintermantel, M.; Schmidt, M.; Tsukahara, Y.; Kajiwara, K.; Kohjiya, S. *Macromol. Rapid Commun.* **1994**, *15*, 279.
- (9) Wintermantel, M.; Fischer, K.; Gerle, M.; Ries, R.; Schmidt, M.; Kajiwara, K.; Urakawa, H.; Wataoka, I. *Angew. Chem., Int. Ed. Engl.* **1995**, *34*, 1472.
- (10) Wintermantel, M.; Gerle, M.; Fischer, K.; Schmidt, M.; Wataoka, I.; Urakawa, H.; Kajiwara, K.; Tsukahara, Y. *Macromolecules* **1996**, *29*, 978.
- (11) Dziezok, P.; Sheiko, S. S.; Fisher, K.; Schmidt, M.; Möller, M. *Angew. Chem., Int. Ed. Engl.* **1997**, *36*, 2812.
- (12) Sheiko, S. S.; Gerle, M.; Fischer, K.; Schmidt, M.; Möller, M. *Langmuir* **1997**, *13*, 5368.
- (13) Wataoka, I.; Urakawa, H.; Kajiwara, K.; Schmidt, M.; Wintermantel, M. *Polym. Int.* **1997**, *44*, 365.
- (14) Prokhorova, S. A.; Sheiko, S. S. *Macromol. Rapid Commun.* **1998**, *19*, 359.
- (15) Terao, K.; Nakamura, Y.; Norisuye, T. *Macromolecules* **1999**, *32*, 711.
- (16) Gerle, M.; Fischer, K.; Roos, S.; Müller, A. H. E.; Schmidt, M. *Macromolecules* **1999**, *32*, 2629.
- (17) Wataoka, I.; Urakawa, H.; Kobayashi, K.; Akaike, T.; Schmidt, M.; Kajiwara, K. *Macromolecules* **1999**, *32*, 1816.
- (18) Djalali, R.; Hugenberg, N.; Fischer, K.; Schmidt, M. *Macromol. Rapid Commun.* **1999**, *20*, 444.
- (19) Stocker, W.; Schürmann, B. L.; Rabe, J. P.; Förster, S.; Lindner, P.; Neubert, I.; Schlüter, A.-D. *Adv. Mater.* **1998**, *10*, 793.
- (20) Förster, S.; Neubert, I.; Schlüter, A. D.; Lindner, P. *Macromolecules* **1999**, *32*, 4043.
- (21) Saariaho, M.; Subbotin, A.; Ikkala, O.; ten Brinke, G. *Macromol. Rapid Commun.* **1999**, in press.
- (22) Saariaho, M.; Ikkala, O.; Szleifer, I.; Erukhimovich, I.; ten Brinke, G. *J. Chem. Phys.* **1997**, *107*, 3267.
- (23) Saariaho, M.; Szleifer, I.; Ikkala, O.; ten Brinke, G. *Macromol. Theor. Simul.* **1998**, *7*, 211.
- (24) Saariaho, M.; Ikkala, O.; ten Brinke, G. *J. Chem. Phys.* **1999**, *110*, 1180.
- (25) Saariaho, M.; Subbotin, A.; Szleifer, I.; Ikkala, O.; ten Brinke, G. *Macromolecules* **1999**, *32*, 4439.
- (26) Rouault, Y.; Borisov, O. V. *Macromolecules* **1996**, *29*, 2605.
- (27) Gallacher, L. V.; Windwer, S. *J. Chem. Phys.* **1966**, *44*, 1139.
- (28) Mazur, J.; McCrackin, F. *Macromolecules* **1977**, *10*, 326.
- (29) Lipson, J. E. G. *Macromolecules* **1991**, *24*, 1327.
- (30) Gauger, A.; Pakula, T. *Macromolecules* **1995**, *28*, 190.
- (31) Rouault, Y. *Macromol. Theory Simul.* **1998**, *7*, 359.
- (32) Khalatur, P. G.; Shirvanyanz, D. G.; Starovoitova, N. Y.; Khokhlov, A. R. *Macromol. Theory Sim.* **1999**, preprint.
- (33) Subbotin, A.; Saariaho, M.; Ikkala, O.; ten Brinke, G. *Macromolecules* **2000**, *33*, 3447.
- (34) Fredrickson, G. H. *Macromolecules* **1993**, *26*, 2825.
- (35) Birshtein, T. M.; Borisov, O. V.; Zhulina, Y. B.; Khokhlov, A. R.; Yurasova, T. A. *Polym. Sci. USSR* **1987**, *29*, 1293.
- (36) Onsager, L. *Ann. N.Y. Acad. Sci.* **1949**, *51*, 627.
- (37) Khokhlov, A. R.; Semenov, A. N. *Physica* **1981**, *108A*, 546.
- (38) Daoud, M.; Cotton, J. P. *J. Physique* **1982**, *43*, 531.
- (39) Semenov, A. *Sov. Phys. JETP* **1985**, *61*, 733.
- (40) Wang, Z.-G.; Safran, S. A. *J. Chem. Phys.* **1988**, *89*, 5323.
- (41) Milner, S. T.; Witten, T. A.; Cates, M. E. *Macromolecules* **1988**, *21*, 2610.
- (42) Milner, S. T.; Wang, Z.-G.; Witten, T. A. *Macromolecules* **1989**, *22*, 489.
- (43) Zhulina, E. B.; Borisov, O. V.; Priamitsyn, V. A. *J. Colloid Interface Sci.* **1990**, *137*, 495.
- (44) Ball, R. C.; Marko, J. F.; Milner, S. T.; Witten, T. A. *Macromolecules* **1991**, *24*, 693.
- (45) Li, H.; Witten, T. A. *Macromolecules* **1994**, *27*, 449.
- (46) Odijk, T. *Macromolecules* **1986**, *19*, 2313.
- (47) Grosberg, A.; Khokhlov, A. *Statistical Physics of Macromolecules*; AIP Press: New York, 1994.
- (48) de Gennes, P.-G. *The Physics of Liquid Crystals*; Clarendon Press: Oxford, England, 1974.